TECHNICAL TRANSACTIONS 7/2017
CZASOPISMO TECHNICZNE 7/2017
MECHANICS
DOI: 10.4467/2353737XCT.17.114.6655

Małgorzata Kowalczyk (kowalczyk@mech.pk.edu.pl)
Faculty of Mechanical Engineering, Cracow University of Technology

Cutting forces during precise turning of NiTi shape memory alloy

Pomiar sił skrawania podczas toczenia precyzyjnego stopu z pamięcią kształtu NiTi

Abstract

The selected indicators of machinability of NiTi based shape memory alloys has been examined. The paper presents research of possibilities of shape memory alloy like low-temperature (austenitic) Ni53Ti47 (Nitinol) with a coated cemented carbide tool, cutting force components (F_f – the feed force, F_p – the passive force, F_c – the main cutting force). In the work, a special attention was paid on the main cutting force components at variable cutting speed (v_c).

Keywords: machinability, Nitinol, precise turning, cutting force

Streszczenie

Wybrane wskaźniki skrawalności stopu z pamięcią kształtu NiTi były przedmiotem badań. W artykule przedstawiono wyniki pomiarów sił skrawania (F_f – siła posuwowa, F_p – siła odporowa, F_c – główna siła skrawania) podczas toczenia precyzyjnego stopu z pamięcią kształtu w fazie nisko temperaturowej (martenzyt) Ni53Ti47 (Nitinol) ostrzem z pokrywanych węglików spiekanych. Szczególną uwagę zwrócono na analizę składowych głównej siły skrawania dla zmiennej prędkości skrawania (v_c).

Słowa kluczowe: skrawalność, Nitinol, toczenie precyzyjne, siły skrawania

1. Introduction

TiNi alloys are an important class of shape memory alloys. In 1938 Greninger and Mooradian1 first observed the shape memory effect for copper-zinc alloys (Cu-Zn) and copper-tin alloys (Cu-Sn). Yet nearly 30 years elapsed until Buehler and his colleagues applied in 1965 for the first patent for a nickel-titanium alloy, called Nitinol, from the Naval Ordnance Laboratory. They exhibit not only shape memory effect SME, but also unusual pseudoelasticity and high damping capacities. These properties along with their superior ductility, fatigue strength, and corrosion resistance, have resulted in many applications.

The microstructure characteristic of Nitinol is that it is in a martensitic phase at lower temperatures, but in an austenitic phase at elevated temperatures. Nitinol exhibits two unique mechanical behaviors: thermal shape memory and superelasticity, which are illustrated in the stress–strain-temperature diagram in Fig. 1.

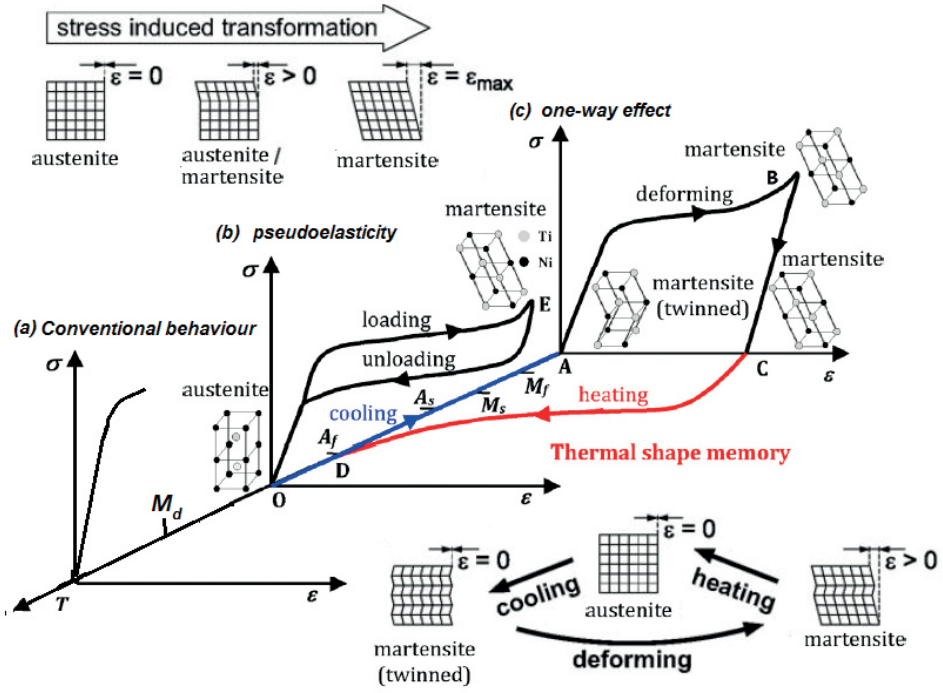

Fig. 1. Temperature dependent stress-strain behaviour of shape memory alloys [4,10]

The phase transformation that occurs in Nitinol is depended on the start and final thermal transitions of the austenite and martensite crystalline phases. It is important to understand the diffusionless transformation to predict the mechanical behavior.

Fig. 1 shows the path that thermal shape memory takes place. Assuming Nitinol initially is in an austenitic state at the origin point O. With no applied stress as Nitinol is cooled

along path O→A below martensite finish temperature (M_f), complete transformation from austenite to martensite (twinned) will occur. The material is deformed through reorientation and detwinning of martensite along path A→B. Then, load releasing on path B→C will cause elastic unloading of the reoriented detwinned martensite and the material stays deformed. On heating above the austenite finish temperature (A_f), the material transforms from martensite to austenite and recovers the pseudoplastic deformation "remembering" its former shape. The austenitic Nitinol can be loaded along the path O→E (Fig. 1) above the austenite finish temperature (A_f) through a stress-induced transformation to martensitic state. A large elastic strain up to 11% can be achieved. Upon unloading along the path →O, the material will transform back to austenitic state and the superelastic deformation will be recovered, demonstrating a hysteresis loop in the stress–strain diagram [5, 13] .

Nitinol, a nearly equiatomic nickel–titanium shape memory alloy, has wide applications in cardiovascular stents, microactuators, and high damping devices. Nitinol alloy is used both in the construction of parts of machines and equipment as well as in medicine. In the first case usually are made portions of the temperature of safety valves, fire detectors, the regulatory systems in the radiators of regulating the flow of fuel and air in carburetors, automatic systems, opening windows in greenhouses, etc. And in the second case of nitinol are made specialized implants for surgery, orthopedics and orthodontics for the treatment of spinal diseases, osteoporosis, fractures rib, malocclusion. Another sphere of application is the arms industry, military and aerospace industry, and industrial robots [2, 4].

In the present study, we aim to investigate the machinability of NiTi alloy by using a mechanical cutting test. In the work, a special attention was paid on the main cutting force components and finish surfaces at variable cutting speed (v_c).

2. Current state of knowledge of the machinability of NiTi alloy

Shape memory alloys are metals, which exhibit two very unique properties, pseudoelasticity and the shape memory effect. The nickel–titanium (NiTi) alloys are one type of these materials; they present additional advantages such as biocompatibility, high ductility, and high strength to weight ratio, good fatigue and corrosion resistance, high damping capacities.

Due to their specific properties NiTi alloys are known to be difficult-to-machine materials particularly by using conventional techniques. Their high ductility, high degree of strain hardening, poor thermal conductivity, very low "effective" elastic modulus and unconventional stress–strain behavior are the main properties responsible for their poor machinability.

As shown in Fig. 2a, machining causes severe tool wear. The machinability of NiTi significantly depends on the cutting speed and feed rate, which should be chosen high enough. Poor chip breaking and the formation of burrs is another problem that can be attributed to the high ductility as well as unconventional stress–strain behavior (Fig. 2b). Despite the optimization of machining parameters, tool wear still remains a problem in machining of these alloys [1, 5, 7–9, 12–13].

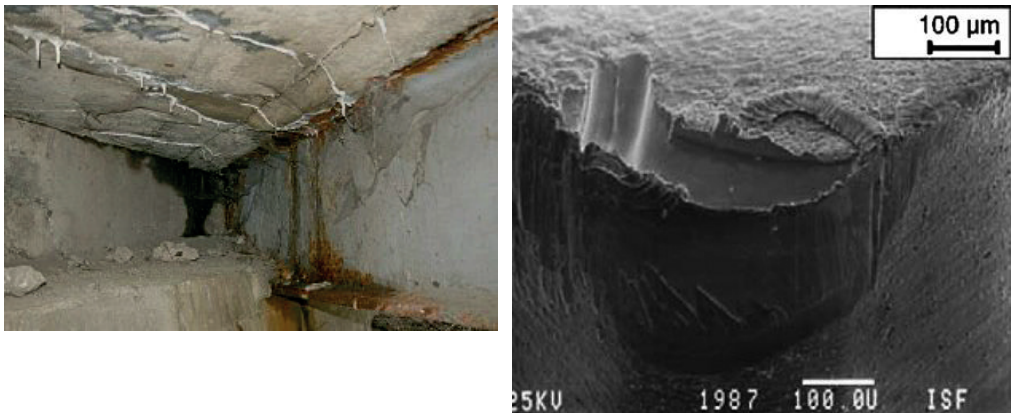

Fig. 2. Major drawbacks in machining NiTi shape memory alloys: a) formation of burrs after turning b) tool wear [4, 13]

3. Experimental procedure

The nominal composition of the examined binary–NiTi shape memory alloy was slightly off-stoichiometry with 52.85 at.% Ni. The austenite finish temperature was, A_f =60°C. Table 1 shows the spectroscopy (EDS) analysis. The thermal and mechanical properties of the material are shown in Table 2, respectively.

Table 1. The spectroscopy (EDS) analysis [own results]

β-*TiNi*		
Element	wt.%	at.%
TiK	42.12	47.15
NiK	57.88	52.85
Total	100	100

Table 2. Physical, mechanical and thermal properties of $Ni_{53}Ti_{47}$ shape memory alloy [6, 10, 13]

β-*TiNi*	**Hardness [HV]**	**Thermal conductivity [W/m·°C]**	**Density [kg/m3]**	**Structure (phase)**	**The tensile Strength [MPa]**	**The tensile Strength Yield [MPa]**	**Modulus of Elasticity [GPa]**
	231	18	6500	hi-temp B2	1364	649	28

A positive 7° clearance 80° rhombic insert with hole made from uncoated carbide was used for research. Fig. 3. The CCGT 060202 – AS insert produced by Iscar has an overall dimension (Fig. 4): d_1 = 2.8 mm, *di* = 6.35 mm, *l* = 6.4 mm, *S* = 2.38 mm. Geometry of tool was following: α_o = 7°; γ_o = 26°; κ_r = 90°. The literature recommends cutting conditions for NiTi alloy; cutting speed v_c = 10–50 m/min; feed rate *f* <0.2 mm/rev; depth of cut a_p <0.5 mm.

The test stand for research of the cutting force components during NiTi alloy turning was consisted of the: precise lathe, work piece (hi – temperature – NiTi), tool holder SCACR 1616K – 06S, insert produced by Iscar, Kistler dynamometer. The values of the cutting force components

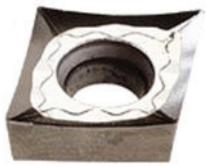

Fig. 3. The photo of insert type CCGT 060202 – AS [14]

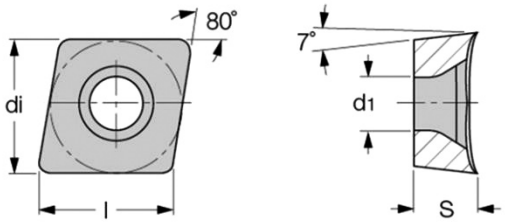

Fig. 4. The overall dimensions of the rhombic insert with hole [14]

(F_f, F_p, F_c) were recorded by the dynamometer and next, the dependence characteristics between the cutting force components and time were in DynoWere software processed.

4. Results of the cutting force components measurements

This work focuses on the study of the cutting force components values (F_f, F_p, F_c) generated during TiNi alloy turning with carbide insert.

The cutting force values for four tests were analyzed and next, the suitable diagrams were generated. The parameters of precise turning process are shown below (Table 3). The diagrams (Fig. 5–6) show dependences between values of the components of cutting forces (F_f, F_p, F_c) and time t [s] for the test1. Also, the tables 4–7 present the average, the lowest and the highest values of cutting forces for selected ranges. The Fig. 6 shows the result of cutting forces components for cutting speed v_c = 50 m/min. In the "range 2" it could be see a sudden increase in cutting forces. This is probably due to formation of burrs after turning (Fig. 2a)

Table 3. The parameters of TiNi alloy turning with carbide insert

Number of research	Cutting speed v_c [m/min]	Feed f [mm/rev]	Depth-of-cut a_p
1	20	0.053	0.2
2	30		
3	40		
4	50		

Table 4. The average, the lowest and the highest cutting force values, for selected ranges during precise turning for cutting speed v_c = 20 m/min

Force component	Average value	Min value	Max value
F_c [N]	43.07	33.87	47.47
F_f [N]	15.92	11.98	17.45
F_p [N]	9.42	8.3	11.01

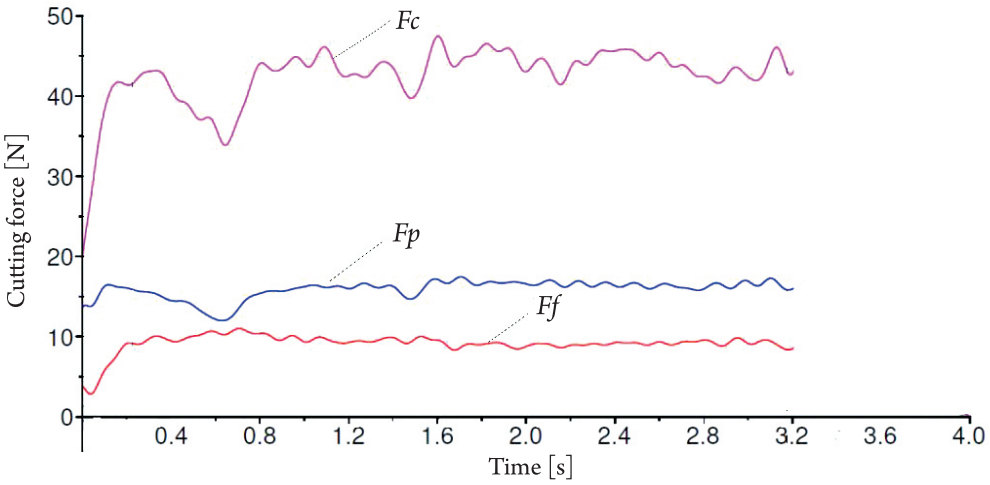

Fig. 5. The result of cutting forces components for cutting speed v_c = 20 m/min

Table 5. The average, the lowest and the highest cutting force values, for selected ranges during precise turning for cutting speed v_c = 30 m/min

Force component	Average value	Min value	Max value
F_c [N]	38.53	26.72	46.8
F_f [N]	14.92	11.92	16.65
F_p [N]	5.81	4.83	6.87

Table 6. The average, the lowest and the highest cutting force values, for selected ranges during precise turning for cutting speed v_c = 40 m/min

Force component	Average value	Min value	Max value
F_c [N]	13.1	11.08	15.54
F_f [N]	19.5	17.77	20.78
F_p [N]	8.87	7.48	10.24

Table 7. The average, the lowest and the highest cutting force values, for selected ranges during precise turning for cutting speed v_c = 50 m/min

Force component	Average value	Min value	Max value
F_c [N]	32.42	30.49	33.69
F_f [N]	9.02	7.75	10.6
F_p [N]	9.69	8.53	10.97

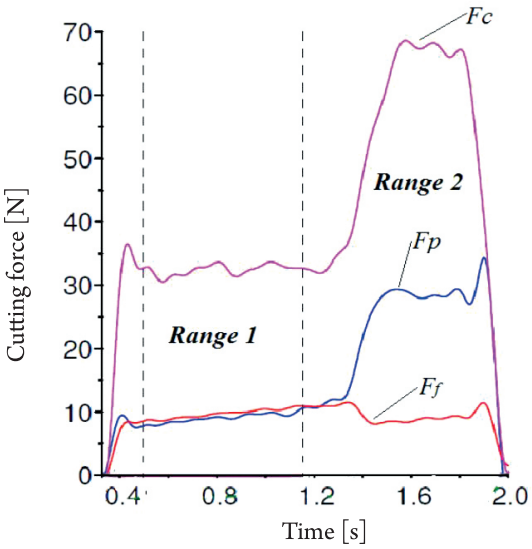

Fig. 6. The result of cutting forces components for cutting speed v_c = 50 m/min

In a next step the influence of the cutting speed on the machinability of NiTi was examined by turning experiments. Figures 7–9 shows the cutting force (F_f – the feed force, F_p – the passive force, F_c – the main cutting force) with respect to its dependence on the cutting speed. The machinability can be classified by three different ranges. At low cutting speeds (v_c = 20 m/min) the main cutting force is the highest (F_c = 44 N – first range – Fig. 7). With increasing cutting speeds the main cutting force decrease. For cutting speeds (v_c = 40 m/min) the feed force is the highest (F_f = 20 N – range 2 – Fig. 8). With increasing cutting speeds the feed force increase also. At high cutting speeds (v_c = 50 m/min) the passive force is the highest (F_p =10 N range 3 – Fig. 9).

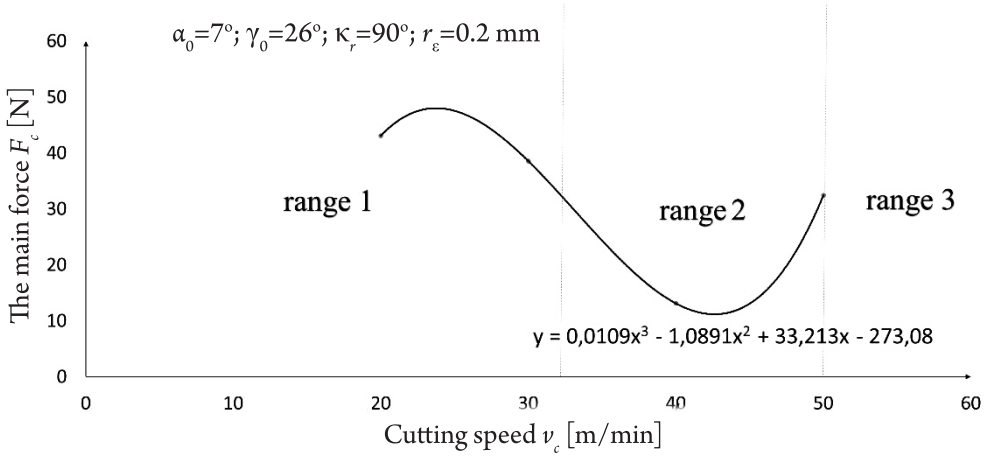

Fig. 7. The main cutting force with respect to its dependence on cutting speed (workpiece: NiTi; cutting parameters: f = 0.053 mm/rev; a_p = 0.2 mm; cutting tool: CCGT 060202 – AS)

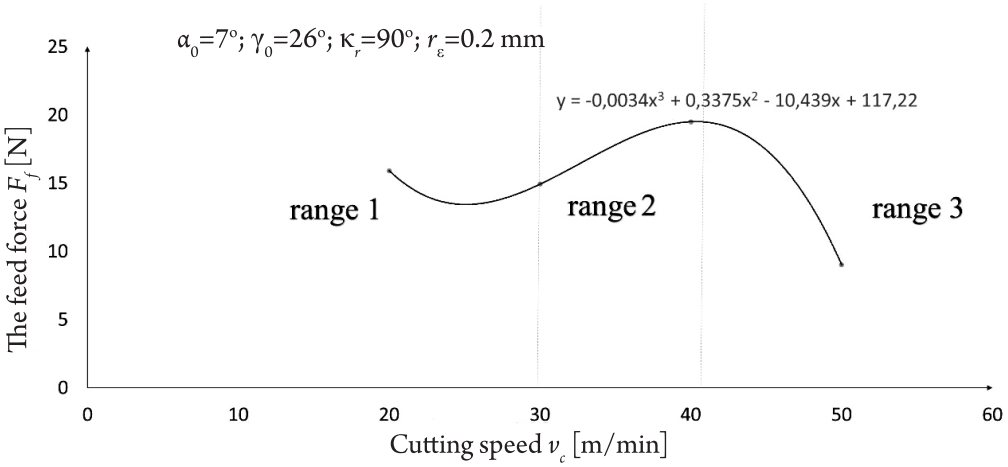

Fig. 8. The feed force with respect to its dependence on cutting speed (workpiece: NiTi; cutting parameters: f = 0.053 mm/rev; a_p = 0.2 mm; cutting tool: CCGT 060202 – AS)

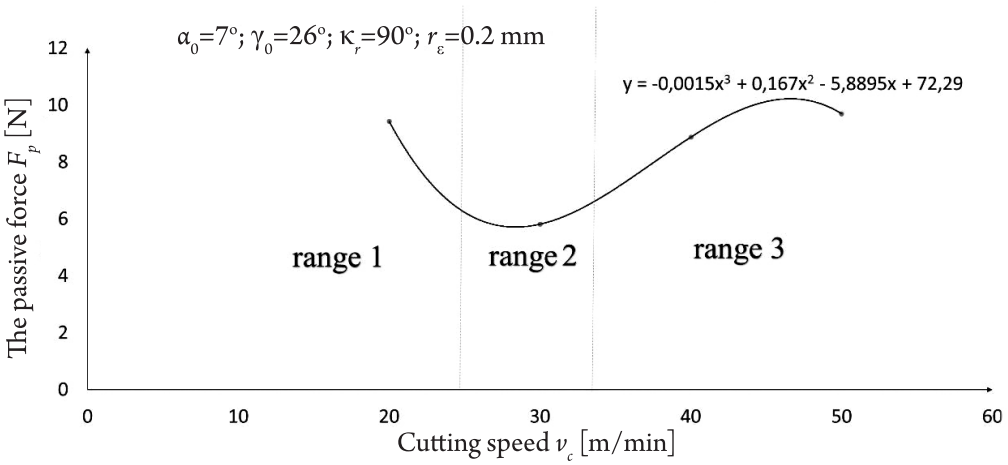

Fig. 9. The passive force with respect to its dependence on cutting speed (workpiece: NiTi; cutting parameters: f = 0.053 mm/rev; a_p = 0.2 mm; cutting tool: CCGT 060202 – AS)

5. Conclusion

Shape memory alloys based on NiTi are difficult to process. Experiments concerning precise turning, to examine the cutting force. The results of obtained values of cutting force during sintered carbides turning for different cutting speeds, constant feed and depth of cut were analyzed. Key findings are as follows:

1) The lowest the main cutting force is for cutting speed v_c = 40m/min (average value: F_c = 13.1 N);
2) The highest the main cutting force is for cutting speed v_c = 20m/min (average value: F_c = 43.07 N);

3) The lowest the feed force is for cutting speed v_c = 50m/min (average value: F_f = 9.02 N);
4) The highest the feed force is for cutting speed v_c = 40m/min (average value: F_f = 19.5 N);
5) The lowest the passive force is for cutting speed v_c = 30m/min (average value: F_p = 5.81 N);
6) The highest the passive force is for cutting speed v_c = 50m/min (average value: F_p = 9.69 N).

Cutting speed has twofold impact on the whole cutting process. First – direct as a ratio of occurring deformations, second – indirect influencing cutting temperature. The indirect impact definitely overrides, that is why the course of the main cutting force during precision turning of NiTi alloy can be described according to Rosenberg and Jeremin basing on so called typical curves [3]. In the speed range v_c = 20 m/min to 40 m/min the main cutting force decreases due to increase of real rake angle (by built up edge) so deformation level decreases. When the cutting speed is getting higher to v_c = 50 m/min main cutting force increases due to vanishing of accretion and decreasing of real rake angle down to the value of rake angle on the cutting edge as well as increase of the friction coefficient. Similar relation were observed in 10 (Fig. 10). Further research would require testing higher cutting speeds.

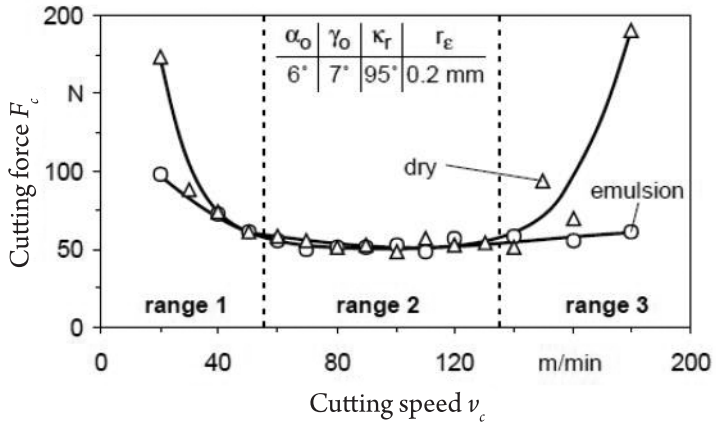

Fig. 10. Cutting force with respect to its dependence on cutting speed and cooling lubricant concept (workpiece: β-NiTi; cutting parameters: f = 0.05 mm/rev; a_p = 0.2 mm; cutting tool: HC TiCN/TiAlN) [10]

References

[1] Biermann D., Kahleyss F., Krebs E., Upmeier T., *A Study on Micro-Machining Technology for the Machining of NiTi: Five-Axis Micro-Milling and Micro Deep-Hole Drilling*, JMEPEG, vol. 20, 2011, 745–751.

[2] Elahinia M. H., Hashemi M., Tabesh M., Bhaduri S. B., *Manufacturing and processing of NiTi implants: A review*, Prog. in Mater. Sci., Vol. 57, 2012, 911–946.
[3] Kaczmarek J., *Podstawy skrawania metali*, PWT., Warszawa 1956.
[4] Guo Y., Klink A., Fu Ch., Snyder J., *Machinability and surface integrity of Nitinol shape memory alloy*, CIRP Annals – Manu. Tech., Vol. 62, 2013, 83–86.
[5] Kaynak Y., Robertson S. W., Karacac H.E., Jawahir I.S., P*rogressive tool-wear in machining of room-temperature austenitic NiTi alloys: The influence of cooling/lubricating, melting, and heat treatment conditions,* J. Mater. Process. Tech., Vol. 215, 2015, 95–104.
[6] Kaynak Y., Karaca H.E., Noebe R.D., Jawahir I.S., *Tool wear analysis in cryogenic machining of NiTi shape memory alloys: A comparison of tool wear performance with dry and MQL machining,* Wear, Vol. 306, 2013, 51–63.
[7] Kłaput J., *Studies of selected mechanical properties of nitinol – shape memory alloy,* Archives of Foundry Engineering, Vol. 10, Issue 3, 2010, 155–158.
[8] Lin H.C., Lin K.M., Chen Y.C., *A study on the machining characteristics of TiNi shape memory alloys*, J. Mater. Process. Tech., Vol. 105, 2000, 327-332.
[9] Piquard R., Acunto A. D, Laheurte P., Dudzinski D., *Micro-end milling of NiTi biomedical alloys, burr formation and phase transformation*, Prec. Eng., Vol. 38, 2014, 356–364.
[10] Weinert K., Petzoldt V., Kotter D., *Turning and Drilling of NiTi Shape Memory Alloys*, CIRP Annals – Manuf. Technol., Vol. 53, Issue 1, 2004, 65–68.
[11] Weinert K., Petzoldt V., *Machining of NiTi based shape memory alloys*, Mater, Sci. and Eng., Vol. 378, 2004, 180–184.
[12] Weinert K., Petzoldt V., *Machining NiTi micro-parts by micro-milling*, Mater, Sci. and Eng., Vol. 481–482, 2008, 672–675.
[13] Wu S.K., Lin H.C., Chen C.C., *A study on the machinability of a Ti 49,6 Ni 50,4 shape memory alloy,* Mater. Letters 40, 1999, 27–3.
[14] http://iscar.pl (access: 03.10.2016).